# LargeBRAT: Complex Backward Reach-Avoid Tubes. An Emergent Collective Behavior Framework.

Olalekan Ogunmolu

Microsoft Research, NYC, 300 Lafayette Street, New York, NY 10012, USA
lekanmolu@microsoft.com.

**Abstract.** Hitherto, the numerical verification of *complex* and *nonlinear* systems via the Isaacs equation (with an overapproximation guarantee of the backward reachable set or tube) has proven elusive owing to the exponential computational complexity associated with resolving value functions on a mesh. In this work, we present a globally isotropic yet locally anisotropic reachable set/tube computational scheme, aimed at computating the backward reach-avoid-tubes (BRATs) of multiple agents interacting over a large state space. This is achieved by resolving the extrema of payoffs on local substructures of the state space whilst preserving desirable global payoff properties. Within the bounds here set, our scheme presents a simple yet effective strategy for designing the verification of *nonlinear systems* for large backward reach-avoid sets or tubes.

## 1 INTRODUCTION

In this paper, we will establish TO-DO: a scheme/general theorem for the practical verification of nonlinear systems via reachability theory. We will resolve the control laws of these systems numerically via Bolza-type objective functionals to realize an aggregated over-approximated backward reach avoid tubes or sets (BRATs) of a large state space. We leverage our understanding of flocking in natural swarms, particularly European starlings (*Sturnus vulgaris*). A motivating example is the verification of cyber-physical systems or CPS, robotic systems requiring dynamical dexterity [27], or systems that do not admit a continuous control law for arriving at an asymptotically stable solution to a dynamical system [9]. Mostly, we will work locally in our formulations, but occasionally will make global remarks.

Differential optimal control theory and games offer a useful paradigm for resolving the safety of multiple agents interacting over a shared space. Both rely on the resolution of the Hamilton-Jacobi-Bellman (HJB) or the Hamilton-Jacobi-Isaacs (HJI) equation. Natural swarms provide clues on efficiently constructing the Hamiltonians and control laws for agents' transients' evolution in a cyberphysical system (CPS) facsimile. Therefore, we draw inspiration from swarm behaviors in verifying the trajectories of combined CPS.

Our goal here is the verification of *complex* and *nonlinear* behavior of *multi-agent autonomous systems* that is robust against a worst-case disturbance, and preserves local safety objectives *under global cohesion goals*. We limit our scope to providing a framework for separately computing the extremals of local payoffs of state space

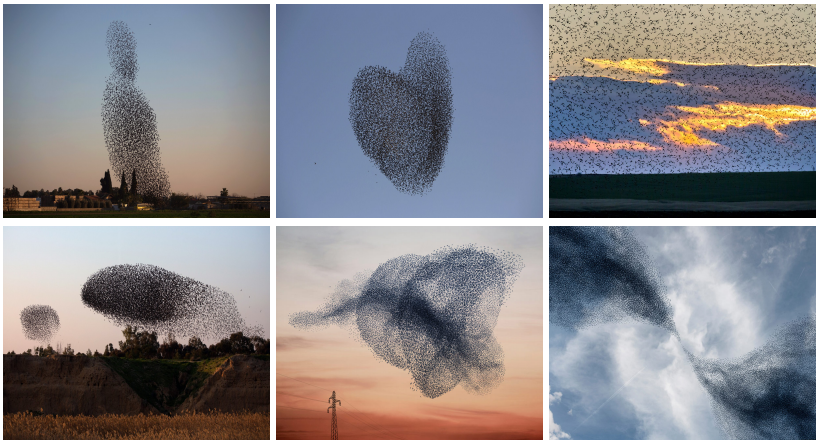

Fig. 1: Starlings murmurations. From the top-left and clockwise. (i) A starlings flock rises into the air, in a dense structure (Reuters/Amir Cohen). (ii) Starlings migrating over an Israeli village (AP Photo/Oded Balilty). (iii) Starlings feeding on laid seeds in the ground in Romania. (iv) Two flocks of migrating starlings (Menahem Kahana/AFP/Getty Images). (v) A concentric conical formation of starlings (Courtesy of The Gathering Site.). (vi) Splitting and joining of a flock of starlings.

substructures over a large range of initial conditions as desired on an interconnected state space, and providing a means for aggregating such locally computed values at the end of each Lax-Friedrichs numerical integration scheme [1, 4]. By properly coordinating local control laws, coordinated influence across workspace regions can be exerted over a wider range.

Local flocks maintain an anisotropic formation, regardless of sparsity of birds within a flock. Thus, intra-flock and inter-flock collision is avoided, attacks are fended off. Given the plethora of possible applications of CPS, questions of robustness, and invariance have received broad attention in the dynamics and control literature lately. For continuous and hybrid systems, the scalability of verification and validation methods is timely in analyzing the safety of complex infrastructure such as ground traffic management systems [15], air traffic management systems [16], flight control systems [5, 17], the invariance of quadrupedal locomotion [18], or adaptive cruise control [19], *inter alia*.

As HJ-type equations, constructed from Bolza-type objective functions, have no classical solution for almost all *practical* problems, stable numerical and computational methods need to be brought to bear in order to produce solutions with (approximately) optimal guarantees. With essentially non-oscillating (ENO) [1] Lax-Friedrichs [2] schemes applied to numerically resolve HJ Hamiltonians [3], we can now obtain numerically *consistent* and *monotone* (viscosity) solutions to HJ-type equations[1] with high accuracy

[1] By consistency, we mean that the numerical approximation to the HJ equation agrees with a defined HJ initial value problem; and by monotonicity, we mean the explicit marching schemes used to resolve the numerical Hamiltonian are a nondecreasing function (for a 1-D case) of each argument of the vector field upon which the state is defined. For more details, see [1, 4].

and precision *on a mesh*. However, resolving HJI solutions on a mesh is not scalable [5–7] owing to the curse of dimensionality [8], as the value function is resolved on a dimension-by-dimension basis on a grid.

Therefore, we consider local control laws in separated partitions of the state space as a plausible procedure for synthesizing the practical verification of nonlinear systems. Through empirical [10–12] and theoretical findings [13], evidence now abounds that in certain natural species that exhibit collective behavior (see Fig. 1), convergence and group cohesion is based on simple topological interaction rules that they use to keep a tab on one another in *local flocks* for collision avoidance, preserving density and structure, flock splitting, vacuole, cordon, and flash expansion [14]. This helps these animals preserve an eye-pleasing local anisotropic synchrony, which taken together among possibly hundreds of thousands of local interactions[2] [14], keep these animals whirling, swooping, and flying in an isotropic formation [10].

Thus, individual agents aggregate into finite flocks, and flock motion is synergized via local topological interactions in order to realize a stable global heading and cohesion [13]. There exists evidence that when an individual within a flock of starlings senses danger (e.g. an attack from a Peregrine Falcon), it changes its course immediately. Owing to the lateral vision in such animals, immediate *nearest neighbors* change course in response. This information is propagated across the entire group of flocks within the fraction of a second [10], resulting in the beautiful formations that we observe c.f. Fig. 1.

While Jadbabaie et al. [13] introduced a graphical formulation based on a switched linear system to demonstrate that nearest neighbor rules cause agents to converge to the same heading, we stick with the nonlinear model of the system and employ *reachability analysis* as a verification tool. We introduce new insights, and computational techniques aimed at solving *practical* problems that cannot be otherwise analytically resolved nor numerically resolved without exploiting state substructures and parallelism. This work is the first to systematically provide a rational separated value function aggregation scheme on local state space substructures in computing *robustly controlled backward reachable tubes (RCBRTs)* [17] for large state spaces. The body of this paper is structured as follows: we introduce common notations and definitions in § 2; § 3 describes the concepts and topics as needed for our proposed scheme in § 4; we present results and insights from experiments in § 5. Lastly, we conclude with remarks in § 6.

## 2 Notations and Definitions.

Let us now introduce the notations that are commonly used in this article. Time variables e.g. $t, t_0, \tau, T$ will always be real numbers. We let $t_0 \leq t \leq t_f$ denote fixed, ordered values of $t$. Vectors shall be column-wise stacked and be denoted by small bold-face letters i.e. $\mathbf{e}, \mathbf{u}, \mathbf{v}$ e.t.c. Matrices will be denoted by bold-math Latin upper case fonts e.g. $\mathbf{T}, \mathbf{S}$. Exceptions: the unit matrix is $I$; and $i, j, k, p$ are indices. We adopt zero-indexing for matrix operations throughout so that if index $i$ corresponds to size $N$, we shall write $i = 0, 1, \cdots, N-1$. Positive, negative, increasing, decreasing e.t.c. shall refer to strict corresponding property.

[2] It has been reported that no birds fly together with greater coordination and complexity than European starlings, with murmurations counting upwards of 750,000 individual birds!

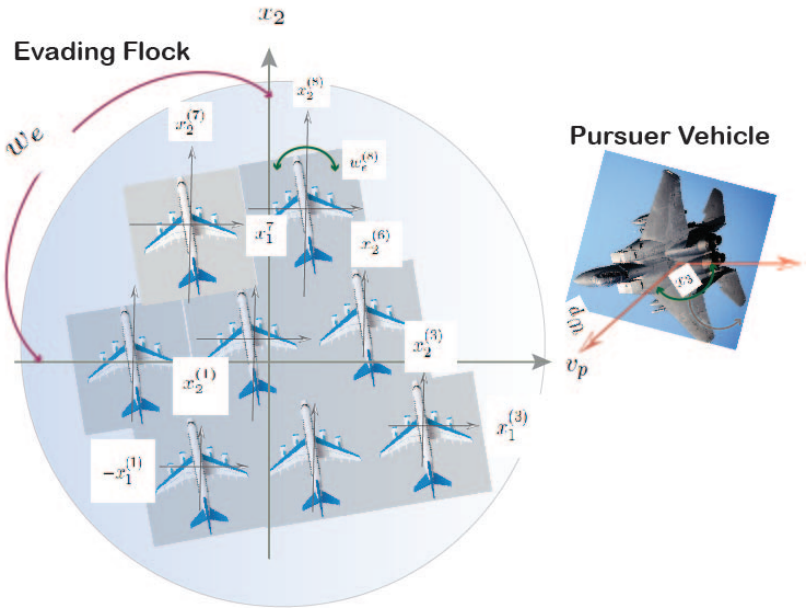


Fig. 2: Illustration of robust heading consensus for a flock. Each agent within the Evading player's control are in relative coordinates w.r.t a pursuing adversary. Each agent (identified by index $i$) within the evading flock is parameterized by three state components: the linear velocities $(\boldsymbol{x}_1^{(i)}, \boldsymbol{x}_2^{(i)})$, and heading $w^{(i)}$. When we need to distinguish an agent within a flock from another flock, we shall use the index of the flock e.g. $j$ as a subscript for a particular e.g. $\boldsymbol{x}_1^{(i)_j}$.

The set $S$ of all $\boldsymbol{x}$ such that $\boldsymbol{x}$ belongs to the real numbers $\mathbb{R}$, and that $\boldsymbol{x}$ is positive shall be written as $S = \{\boldsymbol{x} \,|\, \boldsymbol{x} \in \mathbb{R}, \boldsymbol{x} > 0\}$. The cardinality of $S$ shall be written as $[S]$. We define $\Omega$ as the open set in $\mathbb{R}^n$. To avoid the cumbersome phrase "the state $\boldsymbol{x}$ at time $t$", we will associate the pair $(\boldsymbol{x}, t)$ with the *phase* of the system for a state $\boldsymbol{x}$ at time $t$. Furthermore, we associate the Cartesian product of $\Omega$ and the space $T = \mathbb{R}^1$ of all time values as the *phase space* of $\Omega \times T$. The interior of $\Omega$ is denoted by int $\Omega$; whilst the closure of $\Omega$ is denoted $\bar{\Omega}$. We denote by $\delta\Omega\,(:= \bar{\Omega} \backslash \text{int}\ \Omega)$ the boundary of the set $\Omega$.

Unless otherwise stated, vectors $\boldsymbol{u}(t)$ and $\boldsymbol{v}(t)$ are reserved for admissible control (resp. disturbance) at time $t$. We say $\boldsymbol{u}(t)$ (resp. $\boldsymbol{v}(t)$) is piecewise continuous in $t$, if for each $t$, $\boldsymbol{u} \in \mathcal{U}$ (resp. $\boldsymbol{v} \in \mathcal{V}$), $\mathcal{U}$( resp. $\mathcal{V}$) is a Lebesgue measurable and compact set. At all times, any of $\boldsymbol{u}$ or $\boldsymbol{v}$ will be under the influence of a *player* such that the motion of a state $\boldsymbol{x}$ will be influenced by the will of that player. Our operational domain involves conflicting objectives between various agents e.g. with a heading convergence goal under an external disturbance' influence. For agents that are members of a local coordination group, collision avoidance shall apply so that agents within a local neighborhood cooperate to avoid entropy and preying pursuer(s). Thus, the problem at hand assumes that of a pursuit *game*. And by a game, we do not necessarily refer to a

single game, but rather a *collection of games*. Such a game will terminate when *capture* occurs, that is the distance between players falls below a predetermined threshold.

Each player in a game shall constitute either a pursuer ($\boldsymbol{P}$) or an evader ($\boldsymbol{E}$). The cursory reader should not interpret $\boldsymbol{P}$ or $\boldsymbol{E}$ as controlling a single agent. In complex settings, we may have several pursuers (enemies) or evaders (peaceful citizens). However, when $\boldsymbol{P}$ or $\boldsymbol{E}$ governs the behavior of but one agent, these symbols will denote the agents themselves. Given the various possibilities of outcomes, the question of what is "best" will be resolved by a *payoff*, $\Phi$, whose extremal over a time interval will constitute a *value*, $\boldsymbol{V}$[3]. We adopt Isaac's [20] language so that if the payoff for a game is finite, we shall have a *game of kind*; and for a game with a continuum of payoffs, we shall have *a game of degree*. The *strategy* executed by $\boldsymbol{P}$ or $\boldsymbol{E}$ during a game shall be denoted by $\alpha \in \mathcal{A}$ (resp. $\beta \in \mathcal{B}$). With this definition, a control law e.g. $\boldsymbol{u}^{(i)}$ played by a player e.g. $\boldsymbol{P}$ will affect *agent* $i$; and a collection of agents under $\boldsymbol{P}$'s *willpower* be referred to as a *flock*. We shall refer to an aggregation of flocks on a state space as a *murmuration* [4].

## 3 Reachability for Systems Verification.

A basic characteristic of a control system is to determine the point sets within the state space that are *reachable* with a control input choice. An example objective in *reachability analysis* could be a target ($\mathcal{L}$) protection objective by an evading player from a pursuing player. Our treatment here is a special case of Isaac's homicidal chauffeur's game [20], whereupon $\boldsymbol{P}$ and $\boldsymbol{E}$ travel at constant linear speeds but have different headings, e.g. where the $\boldsymbol{P}$ seeks to drive an evader, $\boldsymbol{E}$, into a target set or tube, $\mathcal{L}$.

### 3.1 Backward Reachability from Differential Games Optimal Control

*Backward reachability* consists in avoiding an unsafe set of states under the worst-possible disturbance and at all times. The verification problem may consist in finding a *set of reachable states* that lie along the trajectories of the solution to a first order nonlinear P.D.E. that originates from some initial state $\boldsymbol{x}_0 = \boldsymbol{x}(0)$ up to a specified time bound, $t = t_f$: *from a set of initial and unsafe state sets, the time-bounded safety verification problem is to determine if there is an initial phase that the solution to the P.D.E. enters an unsafe set*. Backward reachable sets (BRS) or tubes (BRTs) are popularly analyzed as a game of two vehicles with non-stochastic dynamics [21]. Such BRTs possess discontinuity at cross-over points (which exist at edges) on the surface of the tube, and may be non-convex. In general, we seek for a *terminal payoff* $g(\cdot) : \mathbb{R}^n \to \mathbb{R}$ to satisfy

$$|g(\boldsymbol{x})| \leq k, \quad |g(\boldsymbol{x}) - g(\hat{\boldsymbol{x}})| \leq k|\boldsymbol{x} - \hat{\boldsymbol{x}}| \tag{1}$$

for constant $k$ and all $T \leq t \leq 0$, $\hat{\boldsymbol{x}}$, $\boldsymbol{x} \in \mathbb{R}^n$, $\boldsymbol{u} \in \mathcal{U}$ and $\boldsymbol{v} \in \mathcal{V}$. Suppose that the pursuer's mapping strategy (starting at $t$) is $\beta : \bar{\mathcal{U}}(t) \to \bar{\mathcal{V}}(t)$ provided for each

[3] The functional $\boldsymbol{\Phi}$ may be considered a functional mapping from an infinite-dimensional space to the space of real numbers.

[4] The definition of murmurations we use here has a semblance to the murmurations of possibly thousands of starlings observed in nature.

$t \leq \tau \leq T$ and $\boldsymbol{u}, \hat{\boldsymbol{u}} \in \bar{\mathcal{U}}(t)$; then $\boldsymbol{u}(\bar{t}) = \hat{\boldsymbol{u}}(\bar{t})$ a.e. on $t \leq \bar{t} \leq \tau$ implies $\beta[\boldsymbol{u}](\bar{t}) = \beta[\hat{\boldsymbol{u}}](\bar{t})$ a.e. on $t \leq \bar{t} \leq \tau$. *The player* $\boldsymbol{P}$ *is controlling the strategy* $\beta$ *and minimizing*, while the *player* $\boldsymbol{E}$ *is controlling its strategy,* $\alpha$*, and maximizing*.

For any admissible control-disturbance pair $(\boldsymbol{u}(\cdot), \boldsymbol{v}(\cdot))$ and initial phase $(\boldsymbol{x}_0, t_0)$, Crandall [22] and Evan's [3] claim is that there exists a unique trajectory

$$\boldsymbol{\xi}(t) = \boldsymbol{\xi}(t; t_0, \boldsymbol{x}_0, \boldsymbol{u}(\cdot), \boldsymbol{v}(\cdot)) \tag{2}$$

that satisfies

$$\dot{\boldsymbol{x}}(\tau) = f(\tau, \boldsymbol{x}(\tau), \boldsymbol{u}(\tau), \boldsymbol{v}(\tau)) \quad T \leq \tau \leq t, \quad \boldsymbol{x}(t) = \boldsymbol{x}, \tag{3a}$$

where $f(\tau, \cdot, \cdot, \cdot)$ and $\boldsymbol{x}(\cdot)$ are bounded and Lipschitz continuous. This bounded Lipschitz continuity property assures uniqueness of the system response $\boldsymbol{x}(\cdot)$ to controls $\boldsymbol{u}(\cdot)$ and $\boldsymbol{v}(\cdot)$ [23]. a.e. with the property that

$$\boldsymbol{\xi}(t_0) = \boldsymbol{\xi}(t_0; t_0, \boldsymbol{x}_0, \boldsymbol{u}(\cdot), \boldsymbol{v}(\cdot)) = \boldsymbol{x}_0. \tag{4}$$

Read (2): the motion of (3) passing through phase $(\boldsymbol{x}_0, t_0)$ under the action of control $\boldsymbol{u}$, and disturbance $\boldsymbol{v}$, and observed at a time $t$ afterwards.

In backward reachability analysis, the lower value of the differential game [23] is used in constructing an analysis of the backward reachable set (or tube). The differential game's lower value for a solution $\boldsymbol{x}(t)$ that solves (3) for $\boldsymbol{u}(t)$ and $\boldsymbol{v}(t) = \beta[\boldsymbol{u}](\cdot)$ is used in backward reachability analysis, given as

$$\begin{aligned} \boldsymbol{V}^-(\boldsymbol{x}, t) &= \inf_{\beta \in \mathcal{B}(t)} \sup_{\boldsymbol{u} \in \mathcal{U}(t)} \boldsymbol{\Phi}(\boldsymbol{u}, \beta[\boldsymbol{u}]) \\ &= \inf_{\beta \in \mathcal{B}(t)} \sup_{\boldsymbol{u} \in \mathcal{U}(t)} \int_t^T l(\tau, \boldsymbol{x}(\tau), \boldsymbol{u}(\tau), \beta[\boldsymbol{u}](\tau)) d\tau + g\left(\boldsymbol{x}(T)\right). \end{aligned} \tag{5}$$

**Lemma 1.** *The backward reachability problem on the resolution of the infimum-supremum over the non-anticipative strategies of* $\boldsymbol{P}$ *and the controls of* $\boldsymbol{E}$ *with the time of capture resolved as an extremum of the cost functional over a time interval is given by*

$$\frac{\partial \boldsymbol{V}^-}{\partial t}(\boldsymbol{x}, t) + \min\{0, \boldsymbol{H}^-(t; \boldsymbol{x}, \boldsymbol{u}, \boldsymbol{v}, \boldsymbol{V}_{\boldsymbol{x}}^-)\} = 0, \; \boldsymbol{x} \in \mathbb{R}^n, t \in [-T, 0] \tag{6a}$$

$$\boldsymbol{V}^-(\boldsymbol{x}, 0) = g(\boldsymbol{x}), \tag{6b}$$

$$\textit{where } \boldsymbol{H}^-(t; \boldsymbol{x}, \boldsymbol{u}, \boldsymbol{v}, p) = \max_{u \in \mathcal{U}} \min_{v \in \mathcal{V}} \langle f(t; \boldsymbol{x}, \boldsymbol{u}, \boldsymbol{v}), p \rangle, \tag{6c}$$

*and* $p$*, the co-state, is the spatial derivative of* $\boldsymbol{V}^-$ *w.r.t* $\boldsymbol{x}$*. where the vector field* $\boldsymbol{V}_{\boldsymbol{x}}^-$ *is known in terms of the game's terminal conditions so that the overall game is akin to a two-point boundary-value problem.*

Henceforward, for ease of readability, we will remove the minus superscript on the lower value and Hamiltonian (6c).

*Proof.* Lemma 1 is an adaptation of [24]. □

In the sentiment of [24], we say the zero sublevel set of $g(\cdot)$ in (6) i.e. $\mathcal{L}_0 = \{\boldsymbol{x} \in \bar{\Omega} \,|\, g(\boldsymbol{x}) \leq 0\}$, is the *target set* in the phase space $\Omega \times \mathbb{R}$ for a backward reachability problem [25]. This target set[5] can represent the failure set, regions of danger, or obstacles to be avoided e.t.c. in the vectogram. And the *robustly controlled backward reachable tube* for $\tau \in [-T, 0]$[6] is the closure of the open set

$$\mathcal{L}([\tau, 0], \mathcal{L}_0) = \{\boldsymbol{x} \in \Omega \,|\, \exists\, \beta \in \bar{\mathcal{V}}(t)\, \forall\, \boldsymbol{u} \in \mathcal{U}(t), \exists\, \bar{t} \in [-T, 0], \\ \boldsymbol{\xi}(\bar{t}) \in \mathcal{L}_0\},\, \bar{t} \in [-T, 0]\,. \tag{7}$$

Read: the set of states from which the strategies $\beta$ of $\boldsymbol{P}$, and for all controls $\mathcal{U}(t)$ of $\boldsymbol{E}$ imply that we reach the target set within the interval $[-T, 0]$. More specifically, following Lemma 2 of [24], the states in the reachable set admit the following properties w.r.t the value function $\boldsymbol{V}$

$$\boldsymbol{x} \in \mathcal{L}_0 \implies \boldsymbol{V}^-(\boldsymbol{x}, t) \leq 0 \text{ and } \boldsymbol{V}^-(\boldsymbol{x}, t) \leq 0 \implies \boldsymbol{x} \in \mathcal{L}_0. \tag{8}$$

## 4 Materials and Methods.

We locally synthesize the kinematics of agents in a manner amenable to state representation by resolving local payoff extremals – essentially a state space partition induced by a an aggregation of preexisting desired emergent collective behavior from local flocks[7]. Suppose that the local control laws are properly coordinated, the region of the state space across which their coordinated influence might be exerted constitute a larger e.g. manipulability ellipsoid for a dexterous robot manipulation task. We focus on the task verification problem via HJI analysis.

As the verification problem is resolved forward in time, control laws permeate payoff boundaries (semi-permeable surfaces). For each flock, there corresponds local value (cost) functionals that encode a desirable anisotropic density and structural pattern we would like to emerge. These local value functions are constructed by taking into cognizance each agent's topological interaction rule with its neighbors [10]. TO-DO: We leave a thorough evaluation of the nature of the *surfaces*[8] to a future work. TO-DO: These simple tricks allows us to compute large backward reach-avoid tubes that have eluded other scalability methods that have been so far introduced [5, 28, 29].

**Assumptions**: The many interacting subsystems under consideration employ (i) natural units of measurements that are the same for all agents; (ii) kinematics with linear speeds but with a capacity for orientation changes; (iii) intra-flock agent interaction is restricted within unique and distinct state space manifolds; and by agents maneuvering their direction, a kinematic alignment is obtained; (iv) inter-flock interaction occurs when a pursuer is within a threshold of capturing any agent within the murmuration.

[5] Note that the target set, $\mathcal{L}_0$, is a closed subset of $\mathbb{R}^n$ and is in the closure of $\Omega$.

[6] The (backward) horizon, $-T$ is negative for $T > 0$.

[7] Let the cursory reader understand that we use the concept of a flock loosely. The value function could represent a pallete of composed value functions whose extremals resolve local behaviors we would like to emerge over separated local regions of the state space of dextrous drone acrobatics [26], a robot balls juggling task [27] or any parallel task domain verification problem.

[8] Surfaces can be singular, dispersal, or universal in nature [20].

Let us now formalize definitions that will aid the modularization of the problem into manageable forms.

**Definition 1 (Neighbors of an Agent).** *We define the neighbors $\mathcal{N}_i(t)$ of agent $i$ at time $t$ as the set of all agents that lie within a predefined radius, $r_i$, of agent $i$ at time $t$. In every iteration of the game, we update an agent's neighbors as delineated in Algorithm 1.*

**Definition 2.** *We define a flock, $F$, consisting of agents labeled $\{1, 2, \cdots, n\}$ as a collection of agents within a phase space $(\mathcal{X}, T)$ such that all agents within the flock interact with their nearest neighbors in a topological sense.*

*Remark 1.* Every agent within a flock has similar dynamics to that of its neighbor(s). Furthermore, agents travel at the same linear speed, $v$; the angular headings, $w$, however, may be different between agents, seeing we are dealing with a many-bodied system. The state of an agent $i$ within a flock $j$ will be defined as $\boldsymbol{x}^{(i)_j}$ or $\boldsymbol{x}^i_j$. Each agent's continuous-time dynamics, $\dot{\boldsymbol{x}}^{(i)}(t)$, evolves as

$$\begin{bmatrix} \dot{\boldsymbol{x}}_1^{(i)}(t) \\ \dot{\boldsymbol{x}}_2^{(i)}(t) \\ \dot{\boldsymbol{x}}_3^{(i)}(t) \end{bmatrix} = \begin{bmatrix} v(t)\cos \boldsymbol{x}_3^{(i)}(t) \\ v(t)\sin \boldsymbol{x}_3^{(i)}(t) \\ \langle w^{(i)}(t)\rangle_r \end{bmatrix}, \langle w^{(i)}(t)\rangle_r = \frac{1}{1+n_i(t)} \left( w_i(t) + \sum_{j\in\mathcal{N}_i(t)} w_j(t) \right) \tag{9}$$

for agents $i = \{1, 2, 3, ..., n\}$, where $t$ is the continuous-time index, $n_i(t)$ is the number of agent $i$'s neighbors at time $t$, $\mathcal{N}_i(t)$ denotes the sets of labels of agent $i$'s neighbors at time $t$, and $\langle w^{(i)}(t)\rangle_r$ is the average orientation of agent $i$ w.r.t its neighbors at time $t$. Note that for a game where all agents share the same constant linear speed and heading, (9) reduces to the dynamics of a Dubins vehicle in absolute coordinates with $-\pi \leq w^{(i)}(t) < \pi$. The averaging over the degrees of freedom of other agents in (9) is consistent with the *mean field theory*, whereby the effect of all other agents on any one agent is an approximation of a single averaged influence.

**Definition 3 (Payoff of a Flock).** *To every flock $F_j$ (with a finite number of agents $N$) within a murmuration, $j = 1, 2, \cdots, m$ , we associate a payoff, $\boldsymbol{\Phi}$, that is the union of all respective agent's payoffs for expressing the outcome of a desired kinematic behavior.*

Viscosity solutions provide a particular means of finding a unique solution with a clear interpretation in terms of the generalized optimal control problem, even in the presence of stochastic perturbations. Each agent within a flock interacts with a fixed number of neighbors, $n_c$, within a fixed topological range, $r_c$. This topological range is consistent with findings in collective swarm behaviors and it reinforces *group cohesion* [10]. However, we are interested in *robust group cohesion* in reachability analysis. Therefore, we let a pursuer, $\boldsymbol{P}$, with a worst-possible disturbance attack the flock, and we take it that flocks of agents constitute an evading player, $\boldsymbol{E}$. Returning to (9), for a single flock, we now provide a sketch for the HJI formulation for a heading consensus problem.

### 4.1 Framework for Separated Payoffs

We now make the following abstractions to enable our problem formulation. Suppose that a murmuration's global heading is predetermined and each agent $i$ within each flock, $F_j$, $(j = 1, \cdots, n)$ in the murmuration has a constant linear velocity, $v^i$. An agent's orientation is its control input, given by the average of its own orientation and that of its neighbors. Instead of metric distance interaction rules that make agents very vulnerable to predators [10], we resort to a topological interaction rule[9].

What constitutes an agent's neighbors are computed based on empirical findings and studies from the lateral vision of birds and fishes [10, 11, 13] that governs their anisotropic kinematic density and structure. Importantly, starlings' lateral visual axes and their lack of a rear sector reinforces their lack of nearest neighbors in the front-rear direction. As such, this enables them to maintain a tight density and robust heading during formation and flight. The algorithm for computing the nearest neighbors is given in Algorithm 1. On lines 3 and 7 of Algorithm 1, cohesion is reinforced by leveraging the observations above. While the neighbor updates for an agent involve an $O(n^2)$ algorithm in Algorithm 1, we are merely dealing with $6 - 7$ agents at a time in a local flock – making the computational cost measly.

Each agent within a flock $F_j$ interacts with a fixed number of neighbors, $n_c$, within a fixed topological range, $r_c$[10]. This topological range is consistent with findings in collective swarm behaviors and it reinforces *group cohesion* [10]. However, we are interested in *robust group cohesion* in reachability analysis. Therefore, we let a pursuer, $\boldsymbol{P}$, with a worst-possible disturbance attack the flock, and we take it that flocks of agents constitute an evading player, $\boldsymbol{E}$.

### 4.2 Global Isotropy via Local Anisotropy

In this section, methods and results will ci=oincide. It has been observed that structural anisotropy is not merely an effect of a preferential velocity in animal flocking kinematics but rather an explicit effect of the anisotropic interaction character itself. By this theory, agents choose a mutual position on the state space in order to maximize the sensitivity to changes in heading and speed of neighbors as the neighbors' anisotropy is optimized and the scheme of avoiding collisions is vision-based but not related to the eye's structure [10].

Because of the robust group cohesion philosophy, we take it that at least one agent within a flock labeled $j$ is under attack and is in relative coordinates with a pursuer, $\boldsymbol{P}^j$. By averaging the heading of individual agents' orientations with its neighborsc.f. (9), individual agents within a flock can achieve fast response to danger when a pursuer is nearby. TO-DO: In this specialized case, capture does not necessarily occur, because the $\boldsymbol{E}$ and $\boldsymbol{P}$'s speeds and maximum turn radius are equal: if both players start the game with the same initial velocity and orientation, the relative equations of motion show that $\boldsymbol{E}$ can mimic $\boldsymbol{P}$'s strategy by forever keeping the starting radial separation [21]. As such,

[9] With metric distance rules, we will have to formulate the breaking apart of value functions that encode a consensus heading problem in order to resolve the extrema of multiple payoffs; which is typically what we want to mitigate against during real-world autonomous tasks.

[10] The topological range can be set as the distance between the labels of agents in a flock.

**Algorithm 1** Nearest Neighbors For Agents in a Flock.

Given a set of agents $\boldsymbol{a} = \{a_1, a_2, \cdots, a_{n_a} \,|\, [a] = n_a\}$ ▷ $n_a$ agents in a flock $F_k$.
**function** UPDATENEIGHBOR($n$)
  **for** $i$ in $1, \ldots, n$ **do** ▷ Look to the right and update neighbors.
    **for** $j$ in $i+1, \ldots, n$ **do**
      COMPARE_NEIGHBOR($a[i]$, $a[j]$)
    **end for**
    **for** $j$ in $i-1$ down to $0$ **do** ▷ Look to the left and update neighbors.
      COMPARE_NEIGHBOR($a[i]$, $a[j]$)
    **end for**
  **end for**
  **for** each $a_i \in F_k$, $i = 1, \cdots n_a$ **do** ▷ Recursively update agents' headings.
    Update headings according to (9).
  **end for**
**end function**

**function** COMPARE_NEIGHBOR($a_1$, $a_2$) ▷ $(a_1, a_2)$: distinct instances of AGENT.
  **if** $|a_1$.label - $a_2$.label$| < a_1.r_c^1$ ▷ $r_c^n$: agent $n$'s capture radius, $r_c$.
    $a_1$.UPDATE_NEIGHBORS($a_2$) **then**
  **end if**
**end function**

**procedure** AGENT($a_i$, Neighbors={}) ▷ Neighbors: Set of neighbors of this agent.
    ▷ Agent $a_i$ with attributes label $\in \mathbb{N}$, avoid and capture radii, $r_a, r_c$.
  **function** UPDATE_NEIGHBORS(neigh)
    **if** length(neigh)$> 1$ **then** ▷ Multiple neighbors.
      **for** each neighbor of neigh **do**
        UPDATE_NEIGHBORS(neighbor) ▷ Recursive updates.
      **end for**
    **end if**
    Add neigh to Neighbors
  **end function**
**end procedure**

the *barrier* is closed and the *game of kind* is to determine the surface. However, owing to the high-dimensionality of the state space, we cannot resolve this barrier analytically, hence we resort to numerical approximation methods – in particular, we leverage a parallel Lax-Friedrichs integration scheme [30] which we implement in Cupy [31] in order to provide a *consistent* and *monotone* solution to the Hamiltonians of these HJI equations[11].

[11] Consistent solutions to HJ equations are those whose explicit marching schemes via discrete approximations to the HJ IVP agree with the nonlinear HJ solution [4]. Such schemes are said to be *monotone* e.g. on $[-\mathbb{R}, \mathbb{R}]$ if the numerical approximation to the vector field of interest is a nondecreasing function of each argument of the discrete approximation to the vector field.

Therefore, for an agent $i$ within a flock with index $j$ in a murmuration, the equations of motion under attack from a predator (see Fig. 2) in relative coordinates is

$$\begin{bmatrix} \dot{\boldsymbol{x}}_1^{(i)_j}(t) \\ \dot{\boldsymbol{x}}_2^{(i)_j}(t) \\ \dot{\boldsymbol{x}}_3^{(i)_j}(t) \end{bmatrix} = \begin{bmatrix} -v_e^{(i)_j}(t) + v_p^{(j)} \cos \boldsymbol{x}_3^{(i)_j}(t) + \langle w_e^{(i)_j} \rangle_r \boldsymbol{x}_2^{(i)_j}(t) \\ v_p^{(i)_j}(t) \sin \boldsymbol{x}_3^{(i)_j}(t) - \langle w_e^{(i)_j} \rangle_r \boldsymbol{x}_1^{(i)_j}(t) \\ w_p^{(j)}(t) - \langle w_e^{(i)_j}(t) \rangle_r \end{bmatrix} \text{ for } i = 1, \cdots, n_a \tag{10}$$

where $n_a$ is the number of agents within a flock. Read $\boldsymbol{x}_1^{(i)_j}(t)$: the first component of the state of an agent $i$ at time $t$ which belongs to the flock $j$ in the murmuration. In absolute coordinates, the equation of motion for *free agents* is

$$\begin{bmatrix} \dot{\boldsymbol{x}}_1^{(i)_j}(t) \\ \dot{\boldsymbol{x}}_2^{(i)_j}(t) \\ \dot{\boldsymbol{x}}_3^{(i)_j}(t) \end{bmatrix} = \begin{bmatrix} v_e^{(i)_j}(t) \cos \boldsymbol{x}_3^{(i)_j}(t) \\ v_e^{(i)_j}(t) \sin \boldsymbol{x}_3^{(i)_j}(t) \\ \langle w_e^{(i)_j}(t) \rangle_r \end{bmatrix}. \tag{11}$$

As mentioned in Section 2, the evading player at anytime has controls $\{\boldsymbol{u}^1, \boldsymbol{u}^2, \cdots \boldsymbol{u}^n\}$ for agents $i = 1, \cdots, n$ completely under its will. Solving for such complex backward reach-avoid tube is akin to splitting the state space into a number of parts separated by surfaces.

### 4.3 Flock Motion from Aggregated Hamiltonians

We assume that the *value* of a flock heading control (differential game) exists, so that by an extension of Hamilton's principle of least action, the terminal motion of a flock coincide with the extremal of the payoff functional

$$\begin{aligned} \boldsymbol{V}(\boldsymbol{x}, t) = \inf_{\beta^{(1)} \in \mathcal{B}^{(1)}} \sup_{\boldsymbol{u}^{(1)} \in \mathcal{U}^{(\infty)}(t)} \int_{t_0}^{t_f} \boldsymbol{\Phi}^{(1)}(\boldsymbol{u}^{(1)}, \beta^{(1)}[\boldsymbol{u}^{(1)}])dt + g^{(1)}(\boldsymbol{x}(T)) + \\ \cdots + \inf_{\beta^{(n)} \in \mathcal{B}^{(n)}(t)} \sup_{\boldsymbol{u}^{(n)} \in \mathcal{U}^{(n)}(t)} \int_{t_0}^{t_f} \boldsymbol{\Phi}^{(n)}(\boldsymbol{u}^{(n)}, \beta^{(n)}[\boldsymbol{u}^{(n)}])dt + g^{(n)}(\boldsymbol{x}(T)) \end{aligned} \tag{12}$$

where $n$ is the total number of distinct flocks in a murmuration. The resolution of this equation admits a viscosity solution [3] to following variational terminal HJI PDE [24]

$$\sum_{i=1}^{n_f} \left[ \sum_{i=1}^{n_a} \left( \frac{\partial \boldsymbol{V}_i}{\partial t}(\boldsymbol{x}, t) + \min \left[ 0, \boldsymbol{H}^i(\boldsymbol{x}, \boldsymbol{V}_x(\boldsymbol{x}, t)) \right] \right) \right] = 0. \tag{13}$$

In swarms' collective motion, when e.g. a Peregrine Falcon attacks, immediate nearest agents change direction almost instantaneously. And because of the interdependence of the orientations of individual agents with respect to one another, all other agents respond based on the nearest neighbor formulation of (9) and Line 3 of Algorithm 1, every agent in a murmuration responds accordingly. Thus, we only simulate a single attack against a flock within the murmuration to realize robust cohesion.

A pursuer can attack any flock within the murmuration from a distinct surface: a $\boldsymbol{P}$ direction: this side of the surface reached after penetration in the $\boldsymbol{P}-[\boldsymbol{E}-]$ direction is the $\boldsymbol{P}-[\boldsymbol{E}]$ *side* [20]. We attribute the term *in the small* to determine the smooth parts of the singular surface solution when a pursuer attacks, and when they are stitched together into the total solution, we shall describe them as *in the large*. There exists at least one value $\bar{\alpha}$ of $\alpha$ such that if $\alpha = \bar{\alpha}$, no vector in the $\beta$-vectogram[12] penetrates the surface in the $E$-direction. Similar arguments can be made for $\bar{\beta}$ which prevents penetration in the $P$-direction. We adopt [20]'s terminology and call these surfaces semi-permeable surfaces (SPS).

Throughout the game, we assume that the roles of $\boldsymbol{P}$ and $\boldsymbol{E}$ do not change, so that when capture can occur, a necessary condition to be satisfied by the saddle-point controls of the players is the Hamiltonian, $\boldsymbol{H}^i(\boldsymbol{x}, p)$.

**Theorem 1.** *For a flock, $F_j$, the Hamiltonian is the total energy given by a summation of the exerted energy by each agent $i$ so that we can write the main equation or total Hamiltonian of a murmuration as*

$$\boldsymbol{H}(\boldsymbol{x}, p) = \max_{w_e^{(k)_j} \in [\underline{w}_e^j, \bar{w}_e^j]} \min_{w_p^{(k)_j} \in [\underline{w}_p^j, \bar{w}_p^j]} \sum_{j=1}^{n_f} \left( H_a^{(k)_j}(\boldsymbol{x}, p) + \sum_{i=1}^{n_a - 1} H_f^{(i)_j}(\boldsymbol{x}, p) \right) \tag{14}$$

$$\begin{aligned} \boldsymbol{H}_a^{(k)_j}(\boldsymbol{x}, p) = p_1^{(k)_j} \left( v_e^{(k)_j} - v_p^j \cos \boldsymbol{x}_3^{(k)_j} \right) - p_2^{(k)_j} v_p^j \sin \boldsymbol{x}_3^{(k)_j} - \underline{w}_p^j |p_3^{(k)_j}| \\ + \bar{w}_e^j \left| p_2^{(k)_j} \boldsymbol{x}_1^{(k)_j} - p_1^{(k)_j} \boldsymbol{x}_2^{(k)_j} + p_3^{(k)_j} \right|. \end{aligned} \tag{15}$$

*where $n_f$ is the total number of distinct flocks in a murmuration, $n_a$ is the total number of agents within flock $F_j$; $\sum_{i=1}^{n_a-1} \boldsymbol{H}_f^{(i)_j}(\boldsymbol{x}, p)$ is the Hamiltonian of the agents in the evading flock $F_j$, not under attack by $\boldsymbol{P}$, while $\boldsymbol{H}_a^{(k)_j}(\boldsymbol{x}, p)$ is the Hamiltonian for the agent under attack by $\boldsymbol{P}$; $w_e^{(i)_j}$ is the heading of an evader $i$ within a flock $j$ and $w_p^{(j)}$ is the heading of a pursuer aimed at flock $j$; $\underline{w}_e^{(k)_j}$ is the orientation that corresponds to the orientation of the agent with minimum turn radius among all the neighbors of agent $k$, inclusive of agent $k$ at time $t$; similarly, $\bar{w}_e^{(k)_j}$ is the maximum orientation among all of the orientation of agent $k$'s neighbors.*

*Proof.* The complete proof is provided in Appendix A. □

[12] A $\beta-$vectogram is the resulting state space when a the strategy $\beta$ is applied in computing the optimal control law for an agent.

From (15), and for the special case where the linear speeds of the evading agents and pursuer are equal i.e. $v_e^{(i)_j}(t) = v_p(t) = +1m/s$, we have (derived in Appendix A)

$$\begin{aligned}\boldsymbol{H}(\boldsymbol{x}, p) = \sum_{j=1}^{N_f} \sum_{i=1}^{N_a - 1} & p_1^{(i)} \left(1 - \cos \boldsymbol{x}_3^{(i)_j}\right) - p_2^{(i)_j} \sin \boldsymbol{x}_3^{(i)_j} - \underline{w}_p^j |p_3^{(i)_j}| \\ & + \bar{w}_e^j |p_2^{(i)_j} \boldsymbol{x}_1^{(i)_j} - p_1^{(i)_j} \boldsymbol{x}_2^{(i)_j} + p_3^{(i)_j}| + p_1^{(i)_j} v^{(i)_j} \cos \boldsymbol{x}_3 \\ & + p_2^{(i)_j} v^{(i)_j} \sin \boldsymbol{x}_3 + p_3^{(i)_j} \langle w_e^{(i)_j} \rangle_r. \end{aligned} \tag{16}$$

We adopt the essentially non-oscillatory Lax-Friedrichs scheme of [1, 4] in resolving (16). Denote by $(x, y, z)$ a generic point in $\mathbb{R}^3$ so that given mesh sizes $\Delta x,\ \Delta y,\ \Delta z,\ \Delta t > 0$, letters $u, v, w$ will represent functions on the $x, y, z$ lattice $\Delta = \{(x_i, y_j, z_k) : i, j, k \in \mathbb{N}\}$. We define the numerical monotone flux, $\hat{\boldsymbol{H}}^{(i)_j}(\cdot)$, of $\boldsymbol{H}_j^{(i)}(\cdot)$ as

$$\begin{aligned}\hat{\boldsymbol{H}}^{(i)_j}(u^+, u^-, v^+, v^-, w^+, w^-) = \boldsymbol{H}^{(i)_j} & \left(\frac{u^+ + u^-}{2}, \frac{v^+ + v^-}{2}, \frac{w^+ + w^-}{2}\right) \\ & - \frac{1}{2}\left[\alpha_x^{(i)_j}\left(u^+ - u^-\right) + \alpha_y^{(i)_j}\left(v^+ - v^-\right) + \alpha_z^{(i)_j}\left(w^+ - w^-\right)\right] \end{aligned} \tag{17}$$

where

$$\alpha_x^{(i)_j} = \max_{\substack{a \le u \le b \\ c \le v \le d \\ e \le w \le f}} |\boldsymbol{H}_u^{(i)_j}(\cdot)|,\ \alpha_y^{(i)_j} = \max_{\substack{a \le u \le b \\ c \le v \le d \\ e \le w \le f}} |\boldsymbol{H}_v^{(i)_j}(\cdot)|,\ \alpha_z^{(i)_j} = \max_{\substack{a \le u \le b \\ c \le v \le d \\ e \le w \le f}} |\boldsymbol{H}_w^{(i)_j}(\cdot)|. \tag{18}$$

are dissipation coefficients, controlling the level of numerical viscosity in order to realize a stable solution that is physically realistic [4]. Here, the subscripts of $\boldsymbol{H}$ are the partial derivatives w.r.t the subscript variable, and the flux, $\hat{\boldsymbol{H}}(\cdot)$ is monotone for $a \le u^{\pm} \le b, c \le v^{\pm} \le d, e \le w^{\pm} \le f$. We adopt the total variation diminishing Runge-Kutta scheme of [32] in efficiently calculating essentially non-oscillating upwinding finite difference gradients of $\boldsymbol{H}(\cdot)$.

### 4.4 LargeBRAT as a Sequential Composition of Strategy Funnels

The theory we propose here is inspired by the algorithmic notions of robust, self-organizing emergent "behaviors" such as those observed in unactuated masses with passive mechanical guideways [27] or murmurations. Whereas the funneling idea of [27] provides a shifting control law that is only activated in each local partition of the state space when a system's state crosses the boundary towards each portion of the state space, ours is a chained control verification problem that is simultaneously executed across all partitions of the state space based on nearest neighbor rules between agents in order to realize aggressive control and safety verification over as large a state space as possible.

## 5 Experiments

We initialize each flock's agents to distinct positions on the vectogram. All agents share the same linear speed, $v$ and their orientations, $\langle w^{(i)}(t) \rangle_r$, are averaged across every

agent that falls within a nearest neighboring radius, $r_i$ of the label of agent $i$. This is expressed on line 2 of Algorithm 1 . in a flock according to (9). Nearest neighbors are updated according to Algorithm 1. In all our experiments, robust cohesion and anisotropy is reinforced by having an attacking pursuer play against an evading flock as seen in Fig. 2: in every iteration of the game, we randomly pick an agent within a flock, and have the pursuer play a zero-sum against it. Since the orientations of neighboring agents are averaged with that of the singled-out bird, the information is inevitably propagated across the entire flock, and hence the murmuration, so that we can maintain robust cohesion.

At issue is a family of games based on different starting points for local flocks that on the whole constitute a murmuration (see Fig. 3). In starlings, agents move in local flocks of six to seven nearest neighbors [10] in order to preserve cohesion and heading consensus. Therefore, we implicitly compute the payoff for each individual agent in every flock. In this light, a flock's payoff is a union (element-wise minimum f respective payoff points) of the payoff of every agent within it. Therefore, we define the target set and the tube as

$$\begin{aligned}\mathcal{L}_0 &= \left\{\boldsymbol{x} \in \bar{\Omega} | \boldsymbol{V}(\boldsymbol{x}, 0) \leq 0, \boldsymbol{V}(\boldsymbol{x}, 0) = \boldsymbol{V}_1(\boldsymbol{x}_1, 0) \cup \cdots \cup \boldsymbol{V}_n(\boldsymbol{x}_n, 0)\right\}, \\ \mathcal{L}([\tau, 0], \mathcal{L}_0) &= \left\{\boldsymbol{x} \in \bar{\Omega} | \boldsymbol{V}(\boldsymbol{x}, \tau) \leq 0, \boldsymbol{V}(\boldsymbol{x}, 0) = \boldsymbol{V}_1(\boldsymbol{x}_1, 0) \cup \cdots \cup \boldsymbol{V}_n(\boldsymbol{x}_n, 0)\right\}\end{aligned} \tag{19}$$

where $\tau \in [-T, 0]$. A pictorial representation of the zero-level RCBRT of a differential game with six-seven agents in the evading flock (c.f. Fig. 2), constructed from a union of each agent's respective payoff, is depicted in Fig. 3. Each agent's payoff is implicitly defined by a signed distance representation on the state space [33]. Abusing notation and dropping the $i$th superscript for an agent, we construct $\boldsymbol{V}(\cdot)$ as

$$\boldsymbol{V}(\boldsymbol{x}, 0) = \sqrt{\boldsymbol{x}_1^2 + \boldsymbol{x}_2^2} - r_c \tag{20}$$

where $r_c$ is the capture radius, equivalent to the topological range for a flock as reported in [10].

### 5.1 Interagents Spatial Structure

Every local flock has its own payoff, whose target set, together with those of nearest neighbors being interacted with are related by the surfaces. The zero level set of the union of these payoffs constitute the avoid set for a heading consensus. To ensure adequate spatial separation between every agent, we initialize a flock's $j$'s agents, $i = 1, \ldots, n$ on the vectogram in the following way:

$$\boldsymbol{x}^{(i)_j} = \left[r_c \cos(\tfrac{i\pi}{4}),\, r_c \sin(\tfrac{i\pi}{4}),\, h + i\,\delta h\right]^T \tag{21}$$

where $h = 0.1$, $\delta h = 0.05$ and $r_c$ is a collision avoidance radius.

## 6 Conclude

## 7 Acknowledgment

A vote of thanks to Sylvia Herbert of UC San Diego's Mechanical and Aerospace Department and Ian Abraham of Yale University's Mechanical and Aerospace Engineering Department for fruitful discussions in the early development of the ideas reported herein.

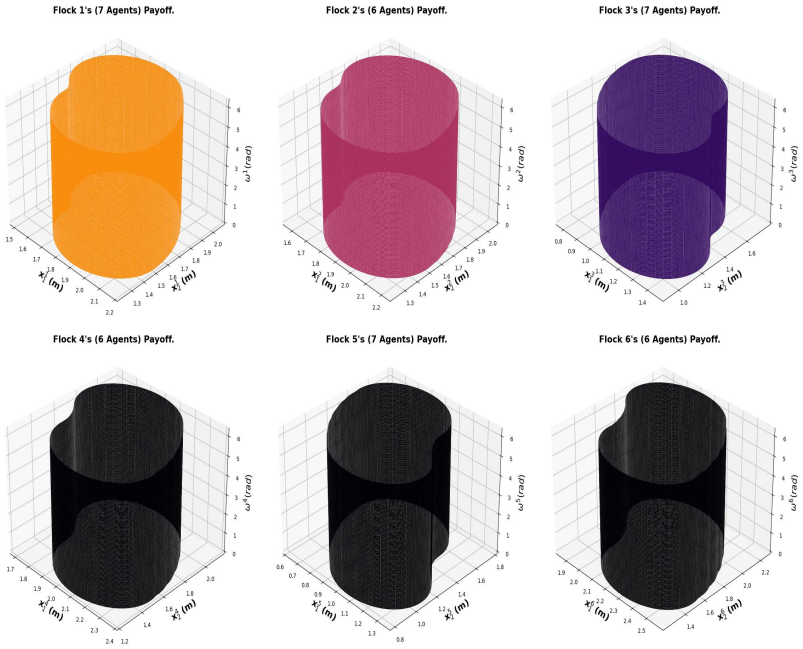


Fig. 3: Illustrative Initial Zero-Level RCBRT for Different Flocks in our Experiment. These are the avoid RCBRTs of the aggregated payoffs of all agents that constitute each flock within a murmuration. (Metric reach radius=$0.2m$, Avoid Radius=$0.2m$).

## A Hamiltonian of a Flock

In this appendix, we provide a derivation for the Hamiltonian of a flock, and by extension, that of a murmuration.

Recall from (15) that the total Hamiltonian of a flock is a sum of the mechanical energy of the free agents in a flock and the individual under attack i.e.

$$\boldsymbol{H}(\boldsymbol{x},p) = \max_{w_e^{(k)^j} \in [\underline{w}_e^j, \bar{w}_e^j]} \min_{w_p^{(k)^j} \in [\underline{w}_p^j, \bar{w}_p^j]} \sum_{j=1}^{n_f} \left( H_a^{(k)^j}(\boldsymbol{x},p) + \sum_{i=1}^{n_a-1} H_f^{(i)^j}(\boldsymbol{x},p) \right) \tag{22}$$

*Proof of Theorem 1.* The Hamiltonian of the free agents is the summation of all the mechanical energy in the system in absolute coordinates i.e.

$$\sum_{i=1}^{n_a-1} H_f^{(i)^j}(\boldsymbol{x},p) = \sum_{i=1}^{n_a-1} \begin{bmatrix} p_1^{(i)^j} & p_3^{(i)^j} & p_3^{(i)^j} \end{bmatrix} \begin{bmatrix} v^{(i)^j} \cos \boldsymbol{x}_3 \\ v^{(i)^j} \sin \boldsymbol{x}_3 \\ \langle w_e^{(i)^j} \rangle_r \end{bmatrix}. \tag{23}$$

We write the Hamiltonian of the free agents in absolute coordinates and the Hamiltonian of the agent under attack in relative coordinates with respect to the pursuer so that (15)

can be re-written as

$$\boldsymbol{H}_a^{(k)_j}(\boldsymbol{x}, p) = -\left(\max_{w_e^{(k)_j} \in [\underline{w}_e^j, \bar{w}_e^j]} \min_{w_p^{(k)_j} \in [\underline{w}_p^j, \bar{w}_p^j]} \begin{bmatrix} p_1^{(k)_j}(t)\, p_2^{(k)_j}(t)\, p_3^{(k)_j}(t) \end{bmatrix} \begin{bmatrix} -v_e^{(k)_j}(t) + v_p^{(j)} \cos \boldsymbol{x}_3^{(k)_j}(t) + \langle w_e^{(k)_j} \rangle_r(t) \boldsymbol{x}_2^{(k)_j}(t) \\ v_p^j(t) \sin \boldsymbol{x}_3^{(k)_j}(t) - \langle w_e^{(k)_j} \rangle_r(t) \boldsymbol{x}_1^{(k)_j}(t) \\ w_p^j(t) - \langle w_e^{(k)_j}(t) \rangle_r \end{bmatrix}\right), \tag{24}$$

where $p_l^{(k)_j}(t)\ |_{l=1,2,3}$ are the adjoint vectors [21]. For the pursuer, its minimum and maximum turn rates are fixed so that we have $\underline{w}_p^j$ as the minimum turn bound of the pursuing vehicle, and $\bar{w}_p^j$ is the maximum turn bound of the pursuing vehicle. Henceforth, we drop the templated time arguments for ease of readability. Rewriting (24), we find that

$$\begin{aligned}
\boldsymbol{H}_a^{(k)_j}(\boldsymbol{x}, p) &= -\left(\max_{w_e^{(k)_j} \in [\underline{w}_e^j, \bar{w}_e^j]} \min_{w_p^{(k)_j} \in [\underline{w}_p^j, \bar{w}_p^j]} \Big[-p_1^{(k)_j} v_e^{(k)_j} + p_1^{(k)_j} v_p^j \cos \boldsymbol{x}_3^{(k)_j} \right. \\
&\left. + p_1^{(k)_j} \langle w_e^{(k)_j} \rangle_r \boldsymbol{x}_2^{(k)_j} + p_2^{(k)_j} v_p^j \sin \boldsymbol{x}_3^{(k)_j} - p_2^{(k)_j} \langle w_e^{(k)_j} \rangle_r \boldsymbol{x}_1^{(i)_j} + p_3^{(k)_j} \left(w_p^j - \langle w_e^{(k)} \rangle_r\right)\Big]\right), \\
&= p_1^{(k)_j} \left(v_e^{(k)_j} - v_p^j \cos \boldsymbol{x}_3^{(k)_j}\right) - p_2^{(k)_j} v_p^j \sin \boldsymbol{x}_3^{(k)_j} \\
&+ \left(\max_{\langle w_e^{(k)_j} \rangle_r \in [\underline{w}_e^j, \bar{w}_e^j]} \min_{w_p^j \in [\underline{w}_p^j, \bar{w}_p^j]} \left[\langle w_e^{(k)_j} \rangle_r \left(p_2^{(k)_j} \boldsymbol{x}_1^{(k)_j} - p_1^{(k)_j} \boldsymbol{x}_2^{(k)_j} + p_3^{(k)_j}\right) - p_3^{(k)_j} w_p^j\right]\right).
\end{aligned} \tag{25}$$

It follows that we have from (25) that

$$\begin{aligned}
\boldsymbol{H}_a^{(k)_j}(\boldsymbol{x}, p) = p_1^{(k)_j} \left(v_e^{(k)_j} - v_p^j \cos \boldsymbol{x}_3^{(k)_j}\right) - p_2^{(k)_j} v_p^j \sin \boldsymbol{x}_3^{(k)_j} - \underline{w}_p^j |p_3^{(k)_j}| \\
+ \bar{w}_e^j \left| p_2^{(k)_j} \boldsymbol{x}_1^{(k)_j} - p_1^{(k)_j} \boldsymbol{x}_2^{(k)_j} + p_3^{(k)_j} \right|.
\end{aligned} \tag{26}$$

In this work, we consider the special case where the linear speeds of the evading agents and pursuer are equal i.e. $v_e^{(i)_j}(t) = v_p(t) = +1m/s$. *A fortiori* the main equation in (25) becomes

$$\begin{aligned}
\boldsymbol{H}_a^{(k)_j}(\boldsymbol{x}, p) = p_1^{(k)_j} \left(1 - \cos \boldsymbol{x}_3^{(k)_j}\right) - p_2^{(k)_j} \sin \boldsymbol{x}_3^{(k)_j} - \underline{w}_p^j |p_3^{(k)_j}| \\
+ \bar{w}_e^j \left| p_2^{(k)_j} \boldsymbol{x}_1^{(k)_j} - p_1^{(k)_j} \boldsymbol{x}_2^{(k)_j} + p_3^{(k)_j} \right|.
\end{aligned} \tag{27}$$

□

## References


1. Osher, S., Shu, C.W.: High-Order Essentially Nonoscillatory Schemes for Hamilton-Jacobi Equations. SIAM Journal of Numerical Analysis **28**(4), 907–922 (1991) 2, 13
2. Crandall, M.G., Majda, A.: Monotone Difference Approximations For Scalar Conservation Laws. Mathematics of Computation **34**(149), 1–21 (1980) 2
3. Evans, L., Souganidis, P.E.: Differential Games And Representation Formulas For Solutions Of Hamilton-Jacobi-Isaacs Equations. Indiana Univ. Math. J **33**(5), 773–797 (1984) 2, 6, 11
4. Crandall, M.G., Lions, P.L.: Two Approximations of Solutions of Hamilton-Jacobi Equations. Mathematics of Computation **43**(167), 1 (1984) 2, 10, 13
5. Herbert, S., Choi, J.J., Sanjeev, S., Gibson, M., Sreenath, K., Tomlin, C.J.: Scalable learning of safety guarantees for autonomous systems using hamilton-jacobi reachability. arXiv preprint arXiv:2101.05916 (2021) 2, 3, 7
6. Bansal, S., Chen, M., Herbert, S., Tomlin, C.J.: Hamilton-Jacobi Reachability: A Brief Overview and Recent Advances. 2017 IEEE 56th Annual Conference on Decision and Control, ACC 2017 pp. 2242–2253 (2018) 3
7. Bajcsy, A., Bansal, S., Bronstein, E., Tolani, V., Tomlin, C.J.: An Efficient Reachability-based Framework for Provably Safe Autonomous Navigation in Unknown Environments. In: 2019 IEEE 58th Conference on Decision and Control (CDC), pp. 1758–1765. IEEE (2019) 3
8. Bellman, R.: Dynamic programming. Princeton University Press (1957) 3
9. Brockett, R.W., et al.: Asymptotic Stability and Feedback Stabilization. Differential Geometric Control Theory **27**(1), 181–191 (1983) 1
10. Ballerini, M., Cabibbo, N., Candelier, R., Cavagna, A., Cisbani, E., Giardina, I., Lecomte, V., Orlandi, A., Parisi, G., Procaccini, A., Viale, M., Zdravkovic, V.: interaction Ruling Animal Collective Behavior Depends On Topological Rather Than Metric Distance: Evidence From A Field Study. Proceedings of the National Academy of Sciences **105**(4), 1232–1237 (2008). DOI 10.1073/pnas.0711437105. URL https://www.pnas.org/content/105/4/1232 3, 7, 8, 9, 14
11. Helbing, D., Farkas, I., Vicsek, T.: Simulating dynamical features of escape panic. Nature **407**(6803), 487–490 (2000) 3, 9
12. Vicsek, T., Czirók, A., Ben-Jacob, E., Cohen, I., Shochet, O.: Novel type of phase transition in a system of self-driven particles. Physical review letters **75**(6), 1226 (1995) 3
13. Jadbabaie, A., Lin, J., Morse, A.S.: Coordination of groups of mobile autonomous agents using nearest neighbor rules. IEEE Transactions on automatic control **48**(6), 988–1001 (2003) 3, 9
14. Haiken, M.: These birds flock in mesmerizing swarms of thousandsbut why is still a mystery. (2021). URL https://www.nationalgeographic.com/animals/article/these-birds-flock-in-mesmerizing-swarms-why-is-still-a-mystery 3
15. Livadas, C., Lynch, N.A.: Formal verification of safety-critical hybrid systems. In: International Workshop on Hybrid Systems: Computation and Control, pp. 253–272. Springer (1998) 2
16. Tomlin, C.J., Lygeros, J., Sastry, S.S.: A game theoretic approach to controller design for hybrid systems. Proceedings of the IEEE **88**(7), 949–970 (2000) 2
17. Mitchell, I.: A Robust Controlled Backward Reach Tube with (Almost) Analytic Solution for Two Dubins Cars. EPiC Series in Computing **74**, 242–258 (2020) 2, 3
18. Ma, W.L., Csomay-Shanklin, N., Kolathaya, S., Hamed, K.A., Ames, A.D.: Coupled control lyapunov functions for interconnected systems, with application to quadrupedal locomotion. IEEE Robotics and Automation Letters **6**(2), 3761–3768 (2021). DOI 10.1109/LRA.2021.3065174 2
19. Ames, A.D., Grizzle, J.W., Tabuada, P.: Control barrier function based quadratic programs with application to adaptive cruise control. Proceedings of the IEEE Conference on Decision and Control **2015-Febru**(February), 6271–6278 (2014). DOI 10.1109/CDC.2014.7040372 2

20. Isaacs, R.: Differential games 1965. Kreiger, Huntigton, NY 5, 7, 12
21. Merz, A.: The game of two identical cars. Journal of Optimization Theory and Applications **9**(5), 324–343 (1972) 5, 9, 16
22. Crandall, M.G., Lions, P.L.: Viscosity solutions of hamilton-jacobi equations. Transactions of the American mathematical society **277**(1), 1–42 (1983) 6
23. Evans, L., Souganidis, P.E.: Differential games and representation formulas for solutions of Hamilton-Jacobi-Isaacs equations. Indiana Univ. Math. J **33**(5), 773–797 (1984) 6
24. Mitchell, I.M., Bayen, A.M., Tomlin, C.J.: A time-dependent Hamilton-Jacobi formulation of reachable sets for continuous dynamic games. IEEE Transactions on Automatic Control **50**(7), 947–957 (2005). DOI 10.1109/TAC.2005.851439 6, 7, 11
25. Mitchell, I.: Games of two identical vehicles. Dept. Aeronautics and Astronautics, Stanford Univ., ... (July), 1–29 (2001). URL http://www.cs.ubc.ca/$\sim$mitchell/Papers/merz.pdf 7
26. Kaufmann, E., Loquercio, A., Ranftl, R., Müller, M., Koltun, V., Scaramuzza, D.: Deep Drone Acrobatics. arXiv preprint arXiv:2006.05768 (2020) 7
27. Burridge, R R and Rizzi, A A and Koditschek, D E: Sequential Composition of Dynamically Dexterous Robot Behaviors. Tech. Rep. 6 (1999) 1, 7, 13
28. Bansal, S., Tomlin, C.J.: DeepReach : A Deep Learning Approach to High-Dimensional Reachability 7
29. Chen, M., Herbert, S.L., Vashishtha, M.S., Bansal, S., Tomlin, C.J.: Decomposition of Reachable Sets and Tubes for a Class of Nonlinear Systems. IEEE Transactions on Automatic Control **63**(11), 3675–3688 (2018). DOI 10.1109/TAC.2018.2797194 7
30. Crandall, M.G., Evans, L.C., Lions, P.L.: Some Properties of Viscosity Solutions of Hamilton-Jacobi Equations. Transactions of the American Mathematical Society **282**(2), 487 (1984). DOI 10.2307/1999247 10
31. Nishino, R., Loomis, C., Hido, S.: Cupy: A numpy-compatible library for nvidia gpu calculations. 31st confernce on neural information processing systems **151** (2017) 10
32. Osher, S., Shu, C.W.: Efficient Implementation of Essentially Non-Oscillatory Shock Capturing Schemes. Tech. rep., NASA Langley Research Center, Hampton, Virginia (1987) 13
33. Osher, S., Fedkiw, R.: Level Set Methods and Dynamic Implicit Surfaces. Applied Mechanics Reviews **57**(3), B15–B15 (2004) 14